Vinay Kumar, *Pardeep Kumar*

EXPERIMENTAL INVESTIGATION ON CURING CONDITIONS OF SELF-COMPACTING GEOPOLYMER CONCRETE INCORPORATING FLY ASH, GGBFS, AND WCP

EKSPERIMENTALNO ISTRAŽIVANJE USLOVA OČVRŠĆAVANJA SAMOZBIJAJUĆEG GEOPOLIMERNOG BETONA KOJI SADRŽI LETEĆI PEPEO, MLEVENU GRANULIRANU ŠLJAKU VISOKE PEĆI I OTPADNI KERAMIČKI PRAH

Originalni naučni rad / Original scientific paper
Rad primljen / Paper received: 17.10.2025
https://doi.org/10.69644/ivk-2026-01-0181

Adresa autora / Author's address:
Department of Civil Engineering, National Institute of Technology, Hamirpur, Himachal Pradesh, India
V. Kumar https://orcid.org/0000-0002-1788-7117 ,
*email: vinay_phdce@nith.ac.in
P. Kumar https://orcid.org/0000-0003-2502-2911

Keywords
- fly ash
- geopolymer
- ambient curing
- oven curing
- strength
- concrete

Ključne reči
- leteći pepeo
- geopolimer
- otvrdnjavanje u uslovima okoline
- otvrdnjavanje u peći
- čvrstoća
- beton

Abstract

Self-compacting geopolymer concrete (SCGPC) is an eco-friendly substitute to traditional Portland cement concrete, known for its lower carbon footprint. This study compares two different types of SCGPC made from fly ash, ground granulated blast furnace slag (GGBFS), and waste ceramic powder (WCP), which are subjected to ambient and oven curing at 60 °C and 80 °C for durations of 24 and 48 hours. The focus has been on the use of WCP in SCGPC, which is essentially industrial waste that can be used in the construction industry. Two batches of SCGPC are prepared: one with 60 % fly ash, 30 % GGBFS, and 10 % WCP (F60G30W10) and another with 70 % fly ash, 30 % GGBFS, and 0 % WCP (F70G30W0). The study investigates the effect of different curing conditions on the fresh state properties, mechanical properties, as well as microstructural characteristics. The results reveal that curing plays a very significant role in enhancing the strength of the SCGPC. In the oven-cured at 80 °C, the compressive strength (CS) of the SCGPC mix F60G30W10 is 33.7 MPa at 28 days, which was 3.37 % higher than that of the oven-cured mix F60G30W0 under similar curing conditions. Scanning electron microscopy (SEM) analyses confirm that the SCGPC microstructure improves with oven curing. X-ray diffraction (XRD) analysis shows that increased curing temperature and WCP content led to higher intensities of mullite, quartzite, CSH gel, and calcite peaks compared to those observed in composite F70G30W0.

Izvod

Samougrađujući geopolimerni beton (SCGPC) je ekološki prihvatljiva zamena za tradicionalni Portland cementni beton, poznat po nižem ugljeničnom otisku. Ova studija upoređuje dve različite vrste SCGPC napravljene od letećeg pepela, mlevene granulirane šljake visoke peći (GGBFS) i otpadnog keramičkog praha (WCP), koji su podvrgnuti očvršćavanju na sobnoj temperaturi i u peći na 60 °C i 80 °C u trajanju od 24 i 48 sati. Fokus je bio na upotrebi WCP u SCGPC-u, koji je u suštini industrijski otpad koji se može koristiti u građevinskoj industriji. Pripremljene su dve serije SCGPC: jedna sa 60 % letećeg pepela, 30 % GGBFS i 10 % WCP (F60G30W10) i druga sa 70 % letećeg pepela, 30 % GGBFS i 0 % WCP-a (F70G30W0). Studija istražuje uticaj različitih uslova očvršćavanja na svojstva svežeg stanja, mehanička svojstva, kao i mikrostrukturne karakteristike. Rezultati pokazuju da očvršćavanje igra veoma značajnu ulogu u povećanju čvrstoće SCGPC. U rerni očvršćen na 80 °C, čvrstoća na pritisak (CS) SCGPC mešavine F60G30W10 bila je 33,7 MPa nakon 28 dana, što je 3,37 % više od čvrstoće kod rerne F60G30W0 pod sličnim uslovima očvršćavanja. Analize skening elektronskom mikroskopijom (SEM) potvrđuju da se mikrostruktura SCGPC poboljšava očvršćavanjem u rerni. Analiza rendgenskom difrakcijom (XRD) pokazuje da povećana temperatura očvršćavanja i sadržaj WCP dovode do većeg intenziteta vrhova mulita, kvarcita, CSH gela i kalcita u poređenju sa onima primećenim kod kompozita F70G30W0.

INTRODUCTION

Concrete is a commonly used construction material that emits greenhouse gases on a vast scale during manufacture, negatively impacting the environment. The utilisation of waste materials for production of construction materials can help prevent the rapid depletion of natural resources. It has been reported that concrete alone is accountable for about 40 % of CO_2 emissions in buildings /1/. Furthermore, up to 20 % of all CO_2 emissions may come from the transportation of material used in the production of concrete /2/. Cement is a crucial and expensive component of concrete. It is estimated to cause CO_2 emissions of about 5-8 % globally /3-5/. The Global Cement and Concrete Association states that 4.2 billion tonnes of cement are currently produced worldwide, and estimates suggest that by 2050, demand will increase to 5.5 billion tonnes /6, 7/. Because of

high carbon footprint associated with cement production, there is a critical need to reduce CO_2 emissions. An effective approach to achieving this is by utilising supplementary cementitious materials, such as GGBFS, WCP, fly ash, metakaolin, silica fume, etc. These materials not only enhance the concrete properties but also decrease the need for landfill disposal and lowered CO_2 emissions, as well as support the sustainability goals /8, 9/.

In 1978, Joseph Davidovits invented geopolymer concrete (GPC) as a substitute for OPC. GPC offers environmental benefits, with an 80 % decrease in CO_2 emissions from source material /4, 10, 11/. GGBFS, WCP, fly ash, metakaolin, silica fume, and other industrial waste products can be used to produce GPC /12-16/. GPC performs similar to OPC in terms of CS, shear strength, split tensile strength, thermal resistance /17/. The primary difference between GPC and OPC concrete lies in their curing processes. In OPC concrete, water is needed for hydration, which leads to strength gain. In GPC, however, a polymerisation reaction occurs when the source material (alumina-silica) reacts with an alkaline activator solution /18/. This reaction forms polymeric chains that act as a binder, with the polycondensation of oligomers forming an aluminosilicate gel that provides durability and strength to the GPC, /19-21/.

SCGPC is a sustainable and environmentally friendly substitute to traditional self-compacting concrete (SCC), using industrial waste materials like, GGBFS, WCP, fly ash, metakaolin, and silica fume instead of OPC. SCGPC retains the beneficial properties of SCC while significantly reducing the carbon footprint of concrete production /22/. A notable feature of SCGPC is its ability to flow and compact under its weight over long distances, filling in congested reinforcement and complex formworks without the need for external vibration /23/. Besides its excellent workability, SCGPC also shows superior mechanical and durability properties, particularly when cured under suitable conditions. Research by /24/ found that increasing GGBFS content and NaOH molarity, along with declining the alkaline liquid-to-binder ratio, reduces the workability of fly ash-GGBFS-based GPC. Conversely, higher molarity, slag concentration, and a lower alkaline liquid to binder ratio significantly increases the CS. Increasing the sodium silicate concentration increases the viscosity of the geopolymer mix, resulting in a lower slump flow value for the GPC.

Curing conditions play a vital role in enhancing SCGPC properties. While ambient curing is convenient and energy-efficient, it may not consistently achieve the desired strength and durability. Oven curing, on the other hand, accelerates the polymerisation process, potentially enhancing mechanical and durability properties /25/. The strength of SCGPC generally increases with an increase in curing temperature, as high curing temperatures accelerate the geopolymerisation process and facilitate its early hardening /26/. Research by /27/ investigated the impact of curing temperatures ranging from 10 to 80 °C on the development of GPC strength, finding that oven-cured mixes gained strength more rapidly than ambient-cured ones. However, ambient-cured GPC, although slower to gain strength initially, showed significant improvements after 28 days /28/. Researcher /29/ studied the shear-bond behaviour of SCGPC with conventional concrete. They found that the CS of ambient-cured SCGPC specimens was 1.61 % higher than that of conventional concrete. In addition, research by /30/ investigates the impact of curing condition on properties of fly ash-based GPC. Their study reveals that the CS of oven-cured GPC specimens at 75 °C is 24.4 % higher than that of conventional concrete at 28 days. In another study, Castel et al. /29/ investigate the bond strength of blended F-class fly ash-GGBFS based GPC with steel reinforcement. Their findings indicate that 48 hours of oven curing at 80 °C is essential to achieve a comparable or better performance than that of OPC-based concrete.

Several studies have investigated the behaviour of SCGPC made from fly ash, GGBFS, and other waste products, as well as their combinations, under ambient and oven curing conditions. However, very limited research has been conducted on their combination with WCP. Much of the study focuses on ambient curing and, to a lesser extent, oven curing conditions. This study seeks to fill this gap by investigating the impact of these curing conditions on SCGPC performance with and without WCP. The performance of the SCGPC is evaluated by the fresh-state properties, compressive strength, split tensile strength, rebound hammer strength, UPV, density, modulus of elasticity, as well as microstructural analysis through SEM, XRD, and Fourier-transform infrared spectroscopy (FTIR) under both curing conditions. This study not only investigates the feasibility of incorporating WCP into SCGPC and the influence of curing conditions on its properties but also provides valuable insights for future sustainable and efficient construction practices, potentially revolutionising concrete production and advancing the industry's sustainability goals.

MATERIALS AND METHODOLOGY

Materials used

To develop the SCGPC, this study utilises class F fly ash, GGBFS, and WCP as binder materials. The fly ash has a particle size of 4.46 microns, specific gravity of 2.07, and bulk density of 770 kg/m^3. The GGBFS has a particle size of 7.0 microns, specific gravity of 2.89, and bulk density of 1100 kg/m^3. The WCP has an average particle size of 12.8 microns, a specific gravity of 2.7, and bulk density of 1300 kg/m^3. Table 1 shows these materials' oxide compositions and percentages, as tested by the supplier company. In the present study, an alkaline activator solution is prepared using sodium silicate and sodium hydroxide (Na_2SiO_3/NaOH) in a ratio of 1.5:1. The molarity of the sodium hydroxide solution is maintained at 12 M based on the previous research /31/. To meet the fresh-state requirements of SCGPC, the high-range water-reducing superplasticizer ‘Auramix 400’

Table 1. Oxides composition of the binders.

Oxides	Fly ash	GGBFS	WCP
SiO_2	54.16	37.73	96.6
Al_2O_3	36.57	14.42	2.19
Cao	2.29	37.34	1.15
Fe_2O_3	1.06	1.11	0.01
LOI	2.94	1.41	0.04
MgO	0.49	8.71	-

is utilised at 6 % by weight of the binders. This superplasticizer has a density of 1.05 g/cm^3, a light-yellow appearance, and low viscosity.

Mix proportion

Two batches of SCGPC, designated F60G30W10 and F70G30W0, are prepared and subjected to ambient temperature and oven curing at 60 °C and 80 °C for durations of 24 and 48 h, respectively. On the basis of previous studies by various researchers on geopolymer concrete, this ratio is chosen to develop SCGPC /32-34/. Our previous work successfully used these ratios to develop SCGPC as they fulfil the EFNARC 2002 standards for SCC /35/. In the current investigation, the activator solution to binder ratio is kept at 0.5, the Na_2SiO_3/NaOH ratio is 1.5:1, and the NaOH solution had a molarity of 12 M. Furthermore, 16 % extra water is added to optimise the mix's workability, strength development, and setting time. However, the inclusion of water beyond a specific threshold caused bleeding and segregation in the mix, leading to a decrease in the concrete's CS /36, 37/. Complete details of mix proportions for SCGPC batches are depicted in Table 2.

Table 2. Mix design proportion of SCGPC.

Materials (kg/m^3)		
Mix designation	F70G30W0	F60G30W10
Fly ash	280	240
GGBFS	120	120
WCP	-	40
Molarity	12	12
NaOH solids	38.4	38.4
Water	81.6	81.6
Sodium silicate	80	80
Superplasticizer % by weight of binder	6	6
Extra water % by weight of binder	16	16
Fine aggregate	1049.4	1049.4
Coarse aggregate	699.6	699.6

*F-Fly ash *G -GGBFS,*W-WCP

Specimen preparation, casting, and testing

A sodium hydroxide solution is prepared one day before casting. Then, it is mixed with sodium silicate solution for one hour before mixing with all the other materials. The dry aggregates are thoroughly mixed with fly ash, GGBFS, and WCP in a mixer for 3 minutes. Subsequently, the alkaline solution is slowly mixed, followed by adding a superplasticizer. The mix is blended for 3 to 5 minutes to achieve homogeneity. Then, it is tested as per the European Federation of Specialist Construction Chemicals and Concrete Systems (EFNARC 2002) /35/ guidelines to evaluate Slump flow, V-funnel, T_{50} cm slump flow, J-ring, and L-box tests. The fresh mix is poured into cubes of 100×100×100 mm for the compressive strength test as per IS 516 (Part 1/Sec 1): 2021 /38/ and 100×200 mm for the split tensile strength test as per IS 516 (Part 1/Sec 1): 2021, /38/. Furthermore, the specimens are left to rest for 24 h at ambient temperature /39, 40/. The SCGPC methodology followed during this work is illustrated in Fig. 1.

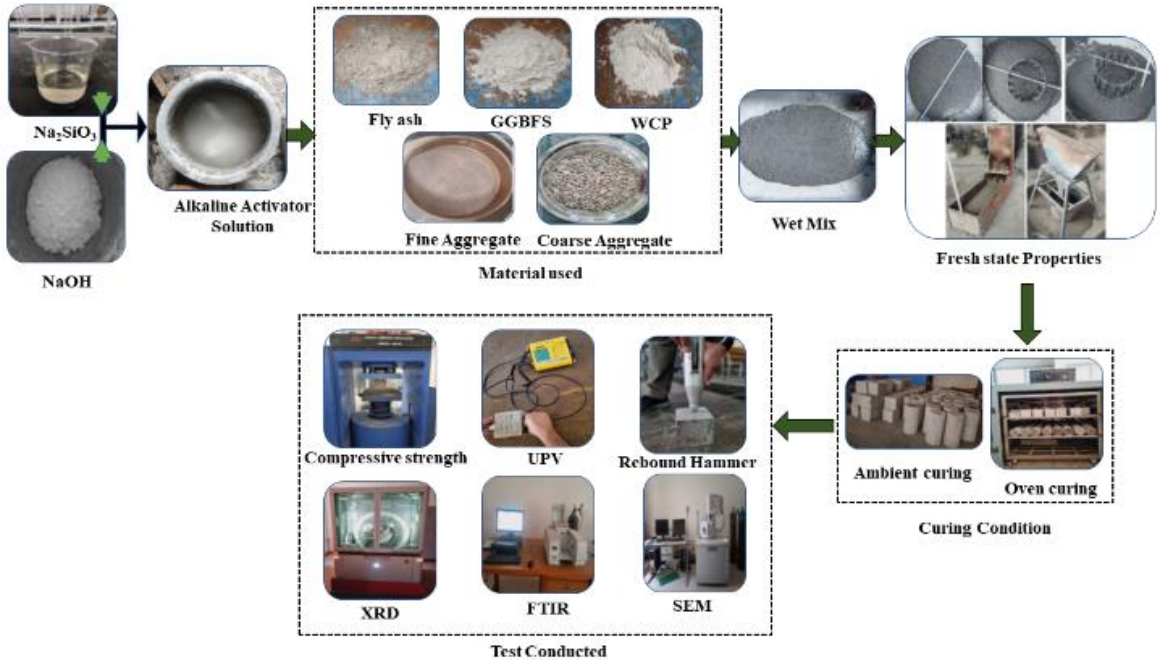

Figure 1. Flowchart of the experimental methodology of SCGPC.

RESULTS AND DISCUSSION

Fresh state properties

The fresh-state properties of the mixture were previously discussed in our article. Figure 2a-e and Table 3 demonstrate the fresh-state properties of SCGPC. The incorporation of WCP as a partial replacement for fly ash, while keeping GGBFS constant, increases the workability of the mixes. This enhancement is primarily ascribed to the increased dosage of superplasticizer rather than the addition of WCP, which has a less pronounced effect. Additionally, the improvement in SCGPC flowability is due to the combined impact of incorporating WCP and the increase in the superplasticizer dosage. Furthermore, it is observed that higher fly ash content reduces the workability of SCGPC due to high-water absorption of fly ash which has a porous structure

/40-42/. This modification affects the rate of chemical reactions. According to EFNARC 2002 /9/ guidelines, the mix F60G30W10 containing 10 % WCP achieves the best results regarding fresh state properties.

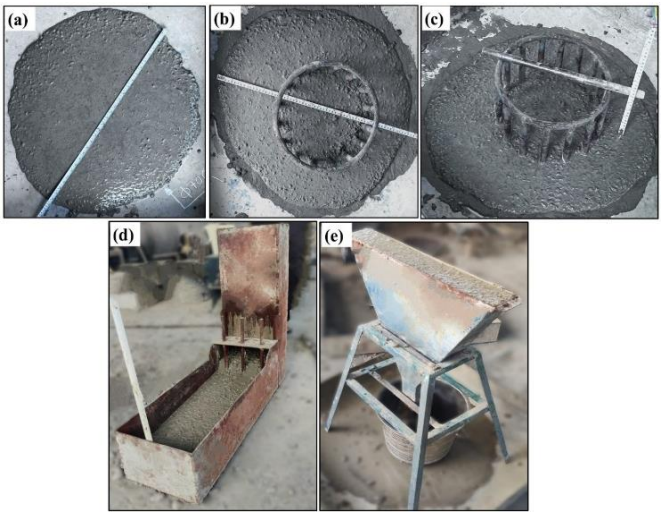

Figure 2. Tested fresh state properties of SCGPC.

Table 3. Experimental results of fresh state properties of SCGPC.

Mix designation	Slump flow (mm)	V-funnel (s)	J-ring flow (mm)	J-ring-Bj (mm)	L-box (H2/H1) ratio	T_{50} (cm) slump flow
F70G30W0 (ambient curing)	684	11	660	9.0	0.98	5
F60G30W10 (ambient curing)	702	12	693	7.0	0.91	5
F70G30W0 (oven curing)	684	11	660	9.0	0.98	5
F60G30W10 (oven curing)	702	12	693	7.0	0.91	5

MECHANICAL PROPERTIES

Compressive strength

The effect of curing conditions on CS of SCGPC composite with F70G30W0 and F60G30W10 is investigated by comparing ambient curing with oven curing at 60 °C and 80 °C for 24 and 48 h. The CS at ages of 3, 7, 28, and 56 days is shown in Table 4 and graphically depicted in Fig. 3. As shown in Fig. 3, the CS of SCGPC F70G30W0 composite at 28 days is 29.0 MPa at 60 °C and 32.6 MPa at 80 °C, compared to 22.4 MPa under ambient curing conditions. The SCGPC composite, cured at 60 °C and 80 °C for 48 h, demonstrates strength improvements of 29.4 % and 45.5 %, respectively, compared to ambient curing. A similar trend is observed for composite F60G30W10 under ambient and oven curing at 60 °C and 80 °C for 24 and 48 h, respectively. The CS of SCGPC composite at 28 days is 32.6 MPa for oven curing at 60 °C and 33.7 MPa for oven curing at 80 °C, compared to 27.3 MPa under ambient curing. For composites cured at 60 °C and 80 °C for 48 h, the strength increases by 19.4 % and 23.4 % at 28 days compared to those under ambient curing conditions.

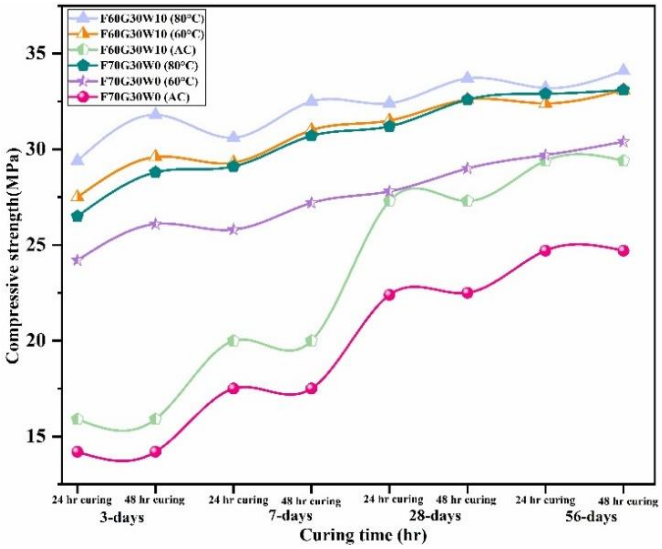

Figure 3. Compressive strength of SCGPC composites F70G30W0 and F60G30W10 at ambient and oven-cured at 60 °C and 80 °C.

Based on these findings, the optimum strength of the oven-cured F60G30W10 composite at 80 °C for 28 days is 33.7 MPa, which is 3.37 % higher than the strength of the F70G30W0 composite under the same curing conditions. This increase in strength is due to the enhanced polymerisation reaction under oven curing, exceeding that of all other composites /43/. Researchers /44, 45/ observed that as the curing temperature increases beyond 80 °C, it leads to a decrease in the CS. Similarly, the CS of F60G30W10 composite at 56 days shows a slight increase in strength compared to the strength observed at 28 days, with a 1.18 % increase compared to oven-cured specimens at 80 °C. Furthermore, the strength of the ambient-cured composite increases gradually over time. In contrast, the oven-cured composite achieves most of its strength within the first 3 days, with only a minor increase in strength observed after that period. The minor increase or decrease in CS after 3 days may be due to the low calcium oxide levels and increased SiO_2 concentration in the binders /46, 47/. Additionally, the slower reaction rates of WCP and fly ash compared to GGBFS partly contribute to these effects, /48/.

Split tensile strength

As depicted in Fig. 4 and Table 4, the split tensile strength of the SCGPC composite F70G30W0 at 28 days is 3.0 MPa at 60 °C and 3.3 MPa at 80 °C, compared to 2.5 MPa under ambient curing conditions. The SCGPC composite cured at 60 °C and 80 °C for 48 h shows an increase in split strength of 20 % and 32 %, respectively, when compared to ambient curing. Similarly, the split tensile strength of the composite F60G30W10 is observed to be 3.6 MPa and 4.3 MPa at 60 °C and 80 °C. This strength increases by 24.1 % and 48.2 %, respectively, at 28 days when compared to ambient curing. On the basis of the test results, it is evident that oven-cured composite, whether F70G30W0 or F60G30W10, achieves sufficient split tensile strength in SCGPC composites compared to ambient curing. The optimum strength of the oven-cured F60G30W10 composite at 80 °C is 4.3 MPa, which is 30.3 % higher than the strength of the F70G30W0 composite under the same curing conditions. This enhance

Table 4. Experimental results of compressive strength and split tensile strength test.

Mix designation	Testing (days)	Curing period (h)	Compressive strength at ambient curing (MPa)	Compressive strength at 60 °C (MPa)	Compressive strength at 80 °C (MPa)	Split tensile strength at ambient curing (MPa)	Split tensile strength at 60 °C (MPa)	Split tensile strength at 80 °C (MPa)
F70G30W0	3	24	14.2	24.2	26.5	1.2	1.6	1.7
		48		26.1	28.1		1.9	2.1
	7	24	17.5	25.8	29.1	1.6	2.0	2.2
		48		27.2	30.7		2.3	2.6
	28	24	22.4	27.8	31.2	2.5	2.8	3.0
		48		29.0	32.6		3.0	3.3
	56	24	24.7	29.7	31.9	2.8	3.2	3.4
		48		30.4	33.1		3.3	3.6
F60G30W10	3	24	15.9	27.5	29.4	1.5	2.2	2.6
		48		29.6	31.8		2.6	2.8
	7	24	20.0	29.3	30.6	1.9	2.5	3.2
		48		31.0	32.5		2.9	3.4
	28	24	27.3	31.5	32.4	2.9	3.3	4.0
		48		32.6	33.7		3.6	4.3
	56	24	29.4	32.4	33.2	3.3	3.7	4.4
		48		33.1	34.1		3.9	4.6

ment can be ascribed to the strong bonding between the CSH gel and filler materials /50/. Moreover, higher curing temperatures accelerate the silica and alumina dissolution, enhance the reactivity of the materials involved, and subsequently improve the overall strength and integrity of the composites, /50/. The strength of SCGPC developed under ambient and oven curing significantly increases with the inclusion of WCP with fly ash and GGBFS compared to the composite without WCP.

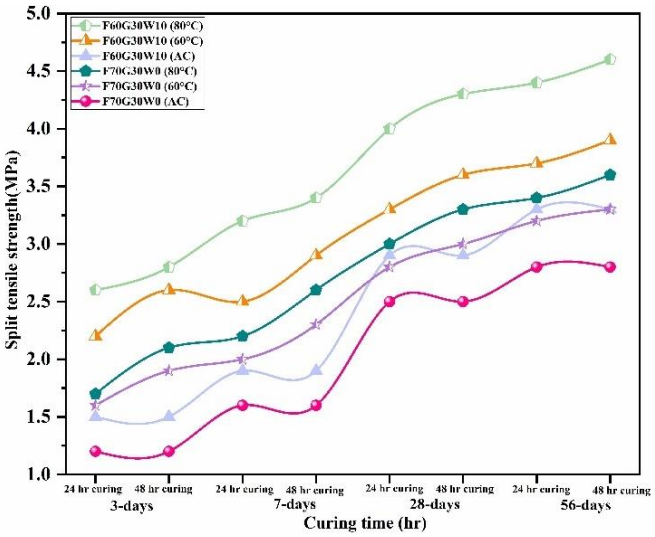

Figure 4. Split tensile strength of SCGPC composites F70G30W0 and F60G30W10 at ambient and oven-cured at 60 °C and 80 °C.

Ultrasonic pulse velocity (UPV)

The UPV values of SCGPC composites F70G30W0 and F60G30W10 are evaluated under both ambient and oven curing at 60 °C and 80 °C for 48 h, with measurements taken at 28 days. For the F70G30W0 composite, the UPV value is 3.45 km/s for the ambient-cured mix, while the oven-cured composite registered 3.80 km/s at 60 °C and 4.05 km/s at 80 °C. In the case of the F60G30W10 composite, the UPV value is 3.77 km/s for ambient curing, 4.1 km/s at 60 °C and 4.39 km/s at 80 °C. According to IS code IS:516-5_4 2020 /51/, concrete quality is classified based on UPV values: excellent above 4.40 km/s, good between 4.40 and 3.75 km/s, doubtful between 3.75 and 3.0 km/s, and poor below 3.0 km/s. Higher UPV values indicate superior concrete quality. The ambient-cured F70G30W0 composite, with a UPV of 3.45 km/s, falls into the doubtful category. The oven-cured F70G30W0 composite, with UPV values of 3.80 km/s and 4.05 km/s at 60 °C and 80 °C, respectively, is classified as good quality concrete according to IS code IS:516-5_4 2020 /51/. Furthermore, the F60G30W10 composite had a UPV of 3.77 km/s under ambient curing and 4.1 km/s and 4.39 km/s under oven curing at 60 °C and 80 °C, respectively, also indicating good quality concrete. These results suggest that ambient-cured composites F70G30W0 and F60G30W10 exhibit lower UPV values compared to their oven-cured counterparts. This may be attributed to increased porosity in the ambient-cured composites, resulting from slower water evaporation and reduced polymerisation rates. The higher porosity leads to the presence of voids, which significantly reduce the composite density and alter the propagation of ultrasonic waves, thereby lowering the UPV values /49, 52, 53/.

Rebound hammer test

Figures 5 and 6 depict the correlation of the CS and compressive strength using the rebound hammer of SCGPC composites F70G30W0 and F60G30W10 under ambient conditions and oven-cured at 60 °C and 80 °C for 24 and 48 h. As depicted in Fig. 5, the composite F70G30W0 shows a decrease of 4.01 % in rebound hammer strength after 48 h of curing at ambient temperature, and a decrease of 1.72 % at 60 °C and 3.37 % at 80 °C, when compared to its CS at 28 days. A linear equation given by $y = 1.0323x - 2.3111y$ is fitted to the results, and a coefficient of determination $R^2 = 0.998$ is obtained. This shows a strong correlation between the two methods. The data points show that the CS measured using the rebound hammer decreases when compared to the CS. Similarly, for the F60G30W10 composite, as shown in Fig. 6, the rebound hammer strength decreases by 4.76 % under ambient temperature, and by 1.84 % and 2.07 % under oven curing at 60 °C and 80 °C, respectively, compared to its CS. A linear equation given by $y = 1.0816x - 3.678y$ is fitted to the results, and a coefficient of determination $R^2 = 0.992$ is obtained. This shows a strong correla-

tion between the two methods. The data points reveal that the rebound hammer CS decreases when compared to the CS. Results show that rebound hammer strength of both composites is lower than their CS. The rebound hammer test measures surface hardness; it may not provide an accurate reflection of the material's overall compressive strength. Typically, the CS values attained from the Rebound Hammer generally differ by ±15 to ±20 % from the actual CS /54, 55/.

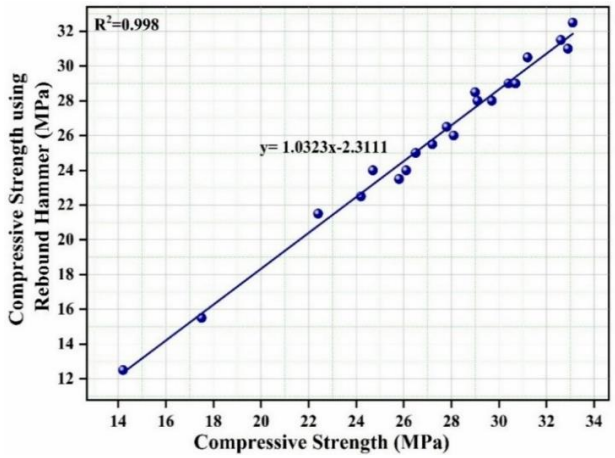

Figure 5. Comparison of test results between compressive strength and rebound hammer strength of composite F70G30W0 at ambient curing and oven-curing.

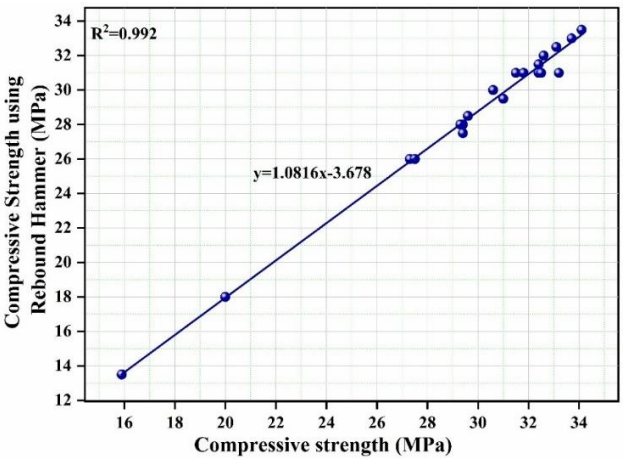

Figure 6. Comparison of test results between compressive strength and rebound hammer strength of composite F70G30W10 at ambient curing and oven-curing.

Density

The density of SCGPC F60G30W10 and F70G30W0 composites is evaluated after a 28-day period at ambient and oven curing at 60 °C and 80 °C for 48 h. As depicted in Fig. 7, the F60G30W10 composite exhibits a density of 2360 kg/m^3 under ambient curing, while oven curing results in densities of 2290 kg/m^3 at 60 °C and 2210 kg/m^3 at 80 °C. Similarly, the F70G30W0 composite records a 2270 kg/m^3 density under ambient curing, corresponding to 2220 kg/m^3 and 2160 kg/m^3 for oven curing at 60 °C and 80 °C. Compared to the F70G30W0 composite, the F60G30W10 shows a 3.96 % higher density under ambient curing, while oven curing at 60 °C and 80 °C leads to density increases of 3.15 % and 2.31 %, respectively. These results indicate that ambient curing leads to a higher density in the WCP-containing composite than oven curing. It can be concluded that, with an increase in curing temperature, the density of both composites decreases, as depicted in Fig. 7. Rahman et al. /56/ reports that the typical density of conventional concrete ranges between 2200 kg/m^3 and 2400 kg/m^3. The density values obtained for F60G30W10 and F70G30W0 composites fall within this range, demonstrating that SCGPC incorporating WCP can achieve comparable density characteristics to conventional concrete.

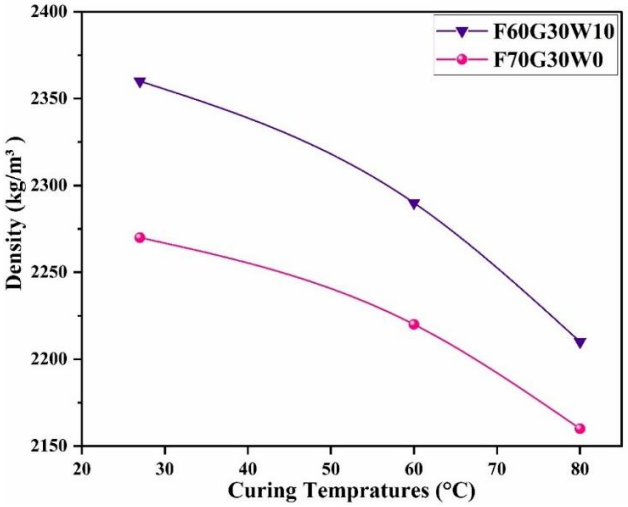

Figure 7. Density of SCGPC composites F60G30W10 and F70G30W0 at ambient curing and oven-curing at 60 °C and 80 °C.

Modulus of elasticity

The stress-strain curve shown in Fig. 8 provides insight into the modulus of elasticity for SCGPC composites under different curing conditions, all of which are attained at a 10 MPa stress level. The modulus of elasticity for the SCGPC composite F60G30W10 is recorded as 23.6 GPa under ambient curing, whereas at 60 °C it increases to 30.1 GPa and at 80 °C it increases to 31.9 GPa. Similarly, the F70G30W0 composite exhibits a modulus of elasticity of 17.3 GPa under ambient curing, which increases to 25.4 GPa at 60 °C and 30.1 GPa at 80 °C. A comparative analysis reveals that the F60G30W10 composite demonstrates a 36.4 % higher modulus of elasticity than the F70G30W0 composite under ambient curing. Additionally, oven-curing at 60 °C and 80 °C results in increases of 18.5 % and 5.98 %, respectively. Furthermore, an increase in modulus of elasticity is observed under ambient temperature and oven-curing conditions for the composites, regardless of whether WCP is included. This enhancement in modulus of elasticity with increasing WCP content may be due to the angular morphology and higher specific surface area of WCP particles, which contribute to improved mechanical interlocking and densification of the matrix. These findings align with the study conducted by /57/, who explored the influence of curing temperature on the modulus of elasticity of geopolymer concrete after 28 days. Their results demonstrate that specimens cured at 50 °C, 70 °C, and 90 °C exhibit increases of 24.4 %, 41.1 %, and 37.7 %, respectively, in the modulus of elasticity compared to those cured at ambient temperature.

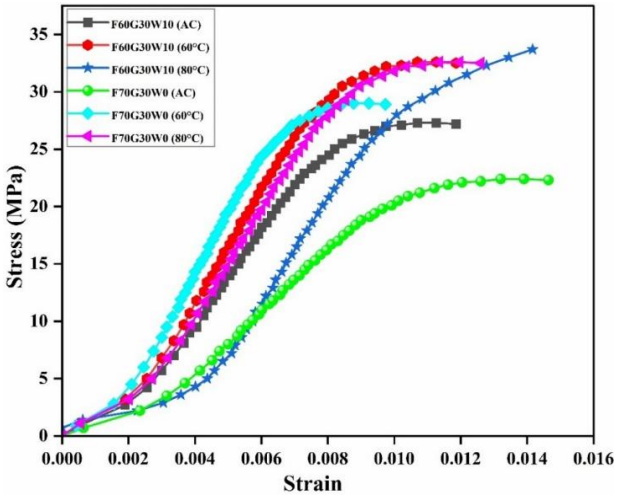

Figure 8. Stress-strain behaviour of SCGPC composites F70G30W0 and F60G30W10 at ambient and oven-cured at 60 °C and 80 °C.

MICROSTRUCTURE ANALYSES

Scanning electron microscope analyses

Figures 9a-f and 10a-f depict the morphology of the 28-day hardened SCGPC F60G30W10 and F70G30W0 composites at ambient temperature and oven cured at 60 °C and 80 °C for 48 h of curing, respectively. The morphology of the composite F70G30W0 at 60 °C, as illustrated in Fig. 9a-b, shows areas with incomplete reactions and the presence of hydration products, as well as large unreacted fly ash and GGBFS particles. In contrast, Fig. 9c-d shows the composite morphology at 80 °C which has a dense microstructure with incompletely reacted GGBFS particles and smaller unreacted fly ash and GGBFS particles compared to the composite at 60 °C. On the other hand, Fig. 9e-f shows that the composite with ambient curing exhibits a small amount of unreacted and partly reacted particles, CSH gel, and a large number of pores. The morphology of the F60G30W10 composite at 60 °C is depicted in Fig. 10a-b, where an increase in WCP enhances the mix's reactivity. Compared to the F70G30W0 composite, smaller unreacted fly ash, GGBFS, WCP particles, and smaller pores are observed at this temperature. Figure 10c-f at 80 °C illustrates that, compared to ambient temperature and oven curing at 60 °C, there is a reduction in particle size of partially reacted fly ash, unreacted GGBFS, and WCP, along with the presence of a small pore. It is found that increasing WCP content while decreasing or fixing the amount of GGBFS adversely affects formation of CSH gel, leading to more incompletely reacted gel, like mullite, and unreacted particles, like quartz /58, 59/. A higher percentage of WCP of more than 10 % increases the silica compounds in the raw materials, which increases the Si/Al ratio to 3.64, as previously reported in our research work /31/. A higher Si/Al ratio hinders further geopolymerisation, increasing unreacted particles, a poorer microstructure, and reduced mechanical strength. If the Si/Al ratio exceeds 3.02, the formation of aluminosilicate gel is reduced, which leads to a reduction in strength /25, 31, 60/. The outcomes show that the composite F60G30W10 at 80 °C exhibits an optimum compressive strength of 33.7 MPa and superior microstructure compared to the F70G30W0 composite at 60 °C, the conditions at 80 °C, and ambient curing.

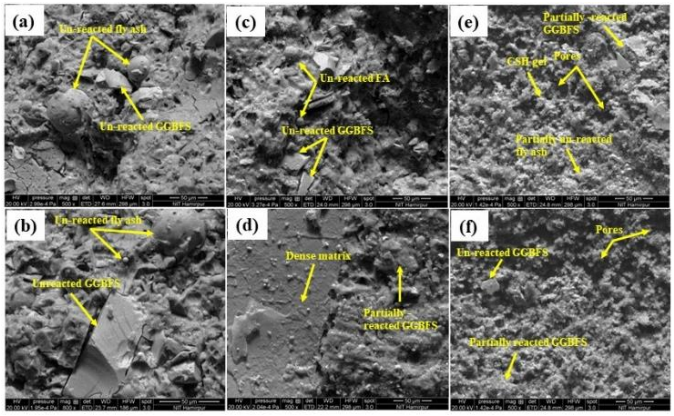

Figure 9. SEM analyses of SCGPC composite F70G30W0 (a, b) at 60 °C (c,d) at 80 °C, and at ambient curing (e, f).

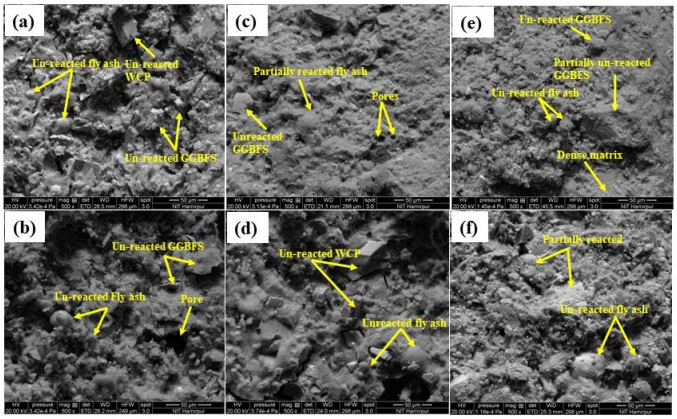

Figure 10. SEM analyses of SCGPC composite F60G30W10 (a, b) at 60 °C (c, d) at 80 °C, and at ambient curing (e, f).

X-ray diffraction

Figure 11 depicts the XRD analyses of F70G30W0 and F60G30W10 composites under ambient temperature, as well as oven curing at 60 °C and 80 °C, respectively. Five quartz peaks at 20.8°, 26.6°, 50.1°, 59.9°, and 68.2° are observed in all composites /31/. Additionally, major quartz peaks at 26.6° and CSH gel peaks at 30.8° are identified in the F60G30W10 compared to the composite with F70G30W0.

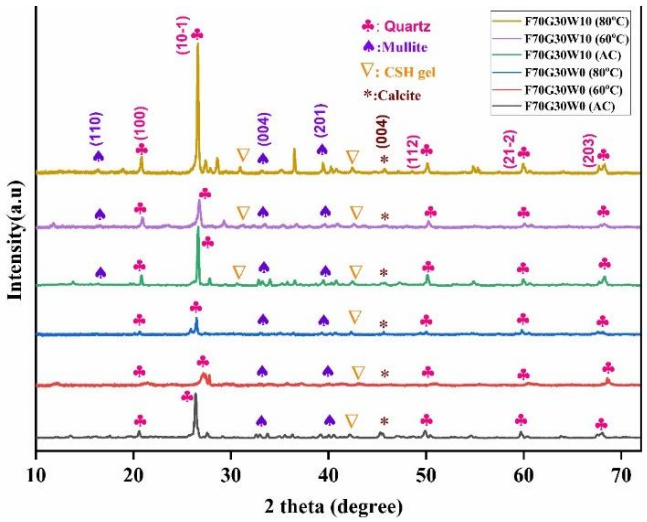

Figure 11. XRD graph of SCGPC composites F70G30W0 and F60G30W10 at ambient and oven-cured at 60 °C and 80 °C.

Figure 11 shows that the composite F60G30W10 at 80 °C exhibits high-intensity peaks for quartz, mullite, and CSH gel. At 60 °C, the phase composition remains similar to that of the 80 °C composite but with slightly lower peak intensities. The XRD graph results show that higher temperatures of the composite F60G30W10 at 80 °C enhance the intensity of crystalline phases such as quartz, mullite, and calcite compared to all other composites. This observation implies that oven curing enhances the crystallinity of the materials, thereby influencing their structural properties.

CONCLUSIONS

This study develops SCGPC using waste ceramic powder at ambient and oven-curing conditions. The SCGPC mixes are assessed for their fresh-state properties, mechanical properties, and microstructural characteristics. Based on the observation, the following conclusions are drawn.

The compressive strength of the composite F60G30W10 increases by 3.37 % after 48 h of curing at 80 °C, 12.4 % after 48 h of curing at 60 °C, and 21.8 % at ambient curing compared to the composite F60G30W0 after 28 days.

In all curing conditions, including ambient curing and oven curing at 60 °C and 80 °C, replacing fly ash with WCP shows a positive effect on the strength of SCGPC. As the content of WCP increases, the compressive and the tensile strength of SCGPC also increase, regardless of the curing temperature.

The addition of WCP enhances the homogeneity of the mix. This is evident from the UPV values for composite F60G30W10, which are higher than those of F70G30W0 at 80 °C.

The rebound hammer strength value of F70G30W0 and F60G30W10 composites at ambient temperature is significantly lower than the actual compressive strength. However, the decrease in rebound hammer strength at oven curing temperatures of 60 °C and 80 °C is less pronounced when compared to the actual compressive strength.

Composites F70G30W0 and F60G30W10 exhibit higher density under ambient curing conditions than those subjected to oven curing at 60 °C and 80 °C.

The modulus of elasticity of the F60G30W10 composite increases by 26.6 %, 19.9 %, and 7.62 % under ambient and oven curing at 60 °C and 80 °C, respectively, compared to the F70G30W0 composite.

The XRD analysis shows that increasing the WCP content and curing temperature leads to higher intensities of mullite, quartzite, CSH gel, and calcite peaks compared to composite F70G30W0. This indicates an increase in strength with an increase in WCP.

The SEM analysis of the SCGPC mix F60G30W10 reveals that increasing the WCP content and curing temperature results in fewer unreacted and partially reacted particles and pores compared to ambient curing.

SEM images reveal the absence of CSH gel formation in oven-cured samples compared to ambient-cured samples in both composites. This may be attributed to the fixed or less concentration of GGBFS, as CaO in GGBFS promotes the formation of gel products, enhancing the density and structural completeness of the composite and thereby improving the mechanical properties of the SCGPC.

REFERENCES

1. Shao, L., Chen, G.Q., Chen, Z.M., et al. (2014), *Systems accounting for energy consumption and carbon emission by building*, Comm. Nonlin. Sci. Num. Sim. 19(6): 1859-1873. doi: 10.1016/j.cnsns.2013.10.003
2. Pacheco, A.A.L., Oliveira, L.S., John, V.M., Angulo, S.C. (2022), *Transportation impact on CO_2 emissions of concrete: a case study in Rio Branco/Brazil*, Rev. IBRACON Estrut. Mater. 15(6): e15609. doi: 10.1590/s1983-41952022000600009
3. Sharma, N.K., Kumar, P., Kumar, S., et al. (2017), *Properties of concrete containing polished granite waste as partial substitution of coarse aggregate*, Constr. Build. Mater. 151: 158-163. doi: 10.1016/j.conbuildmat.2017.06.081
4. Singh, N.B., Middendorf, B. (2020), *Geopolymers as an alternative to Portland cement: An overview*, Constr. Build. Mater. 237: 117455. doi: 10.1016/j.conbuildmat.2019.117455
5. Liu, N., Wang, Y., Bai, Q., et al. (2022), *Road life-cycle carbon dioxide emissions and emission reduction technologies: A review*, J Traffic Transp. Eng. 9(4): 532-555. doi: 10.1016/j.jtte.2022.06.001
6. Gok, S.G., Sengul, O. (2020), *The use of waste glass as an activator in alkali-activated slag mortars*, In: Proc. of the Instit. Civ. Eng.: Eng. Sustain. 174(3): 120-130. doi: 10.1680/jensu.19.00070
7. Bhagath Singh, G.V.P., Durga Prasad, V. (2024), *Environmental impact of concrete containing high volume fly ash and ground granulated blast furnace slag*, J Clean. Prod. 448: 141729. doi: 10.1016/j.jclepro.2024.141729
8. Knight, K.A., Cunningham, P.R., Miller, S.A. (2023), *Optimizing supplementary cementitious material replacement to minimize the environmental impacts of concrete*, Cem. Concr. Compos. 139: 105049. doi: 10.1016/j.cemconcomp.2023.105049
9. Asadollahfardi, G., Katebi, A., Taherian, P., Panahandeh, A. (2021), *Environmental life cycle assessment of concrete with different mixed designs*, Int. J Constr. Manag. 21(7): 665-676. doi: 10.1080/15623599.2019.1579015
10. Mikulčić, H., Klemeš, J.J., Vujanović, M., et al. (2016), *Reducing greenhouse gasses emissions by fostering the deployment of alternative raw materials and energy sources in the cleaner cement manufacturing process*, J Clean. Prod. 136(Part B): 119-132. doi: 10.1016/j.jclepro.2016.04.145
11. La Scalia, G., Saeli, M., Adelfio, L., Micale, R. (2021), *From lab to industry: Scaling up green geopolymeric mortars manufacturing towards circular economy*, J Clean. Prod. 316: 128164. doi: 10.1016/j.jclepro.2021.128164
12. Yang, S., Zhao, R., Ma, B., et al. (2023), *Mechanical and fracture properties of fly ash-based geopolymer concrete with different fibers*, J Build. Eng. 63(Part A): 105281. doi: 10.1016/j.jobe.2022.105281
13. Huseien, G.F., Sam, A.R.M., Shah, K.W., et al. (2019), *Properties of ceramic tile waste based alkali-activated mortars incorporating GBFS and fly ash*, Constr. Build. Mater. 214: 355-368. doi: 10.1016/j.conbuildmat.2019.04.154
14. Albidah, A., Alqarni, A.S., Abbas, H., et al. (2022), *Behavior of Metakaolin-Based geopolymer concrete at ambient and elevated temperatures*, Constr. Build. Mater. 317: 125910. doi: 10.1016/j.conbuildmat.2021.125910
15. Somna, R., Saowapun, T., Somna, K., Chindaprasirt, P. (2022), *Rice husk ash and fly ash geopolymer hollow block based on NaOH activated*, Case Stud. Constr. Mater. 16: e01092. doi: 10.1016/j.cscm.2022.e01092
16. Jena, S., Panigrahi, R. (2022), *Performance evaluation of sustainable geopolymer concrete produced from ferrochrome slag and silica fume*, Eur. J Environm. Civ. Eng. 26(11): 5204-5220. doi: 10.1080/19648189.2021.1886179

17. Wu, X., Shen, Y., Hu, L. (2022), *Performance of geopolymer concrete activated by sodium silicate and silica fume activator*, Case Stud. Constr. Mater. 17: e01513. doi: 10.1016/j.cscm.2022.e01513
18. Kanagaraj, B., Anand, N., Kiran, T., et al. (2022) *Experimental investigation on fresh and hardened properties of geopolymer concrete blended with recycled concrete aggregate*, Ind. Concrete J, 96(1): 29-41.
19. Almutairi, A.L., Tayeh, B.A., Adesina, A., et al. (2021), *Potential applications of geopolymer concrete in construction: A review*, Case Studies Constr. Mater. 15: e00733. doi: 10.1016/j.cscm.2021.e00733
20. Tang, Z.Q., de Souza, F.B., Mulder, R.J., et al. (2022), *Multi-step nucleation and growth mechanism of aluminosilicate gel observed by cryo-electron microscopy*, Cem. Concr. Res. 159: 106873. doi: 10.1016/j.cemconres.2022.106873
21. Verma, N.K., Meesala, C.R., Kumar, S. (2023), *Developing an ANN prediction model for compressive strength of fly ash-based geopolymer concrete with experimental investigation*, Neural Comput. Appl. 35(14): 10329-10345. doi: 10.1007/s00521-023-08237-1
22. Parathi, S., Nagarajan, P., Pallikkara, S.A. (2021), *Ecofriendly geopolymer concrete: a comprehensive review*, Clean Technol. Environ. Policy, 23: 1701-1713. doi: 10.1007/s10098-021-02085-0
23. Dey, S., Kumar, V.V.P., Goud, K.R., Basha, S.K.J. (2021), *State of art review on self compacting concrete using mineral admixtures*, J Build. Pathol. Rehab. 6(1): 18. doi: 10.1007/s41024-021-00110-9
24. Fang, G., Ho, W.K., Tu, W., Zhang, M. (2018), *Workability and mechanical properties of alkali-activated fly ash-slag concrete cured at ambient temperature*, Constr. Build. Mater. 172: 476-487. doi: 10.1016/j.conbuildmat.2018.04.008
25. Patel, Y.J., Shah, N. (2018), *Development of self-compacting geopolymer concrete as a sustainable construction material*, Sust. Environ. Res. 28(6): 412-421. doi: 10.1016/j.serj.2018.08.004
26. Ezuldin, N.Y., Raoof, S.M., Alattar, A.A., Hamada, H. (2025), *Factors affecting durability properties of GPC: A review*, Res. Eng. Struct. Mater. 11(1): 21-43. doi: 10.17515/resm2024.145ma0109rv
27. Rovnaník, P., Bayer, P., Rovnaníková, P. (2013), *Characterization of alkali activated slag paste after exposure to high temperatures*, Constr. Build. Mater. 47: 1479-1487. doi: 10.1016/j.conbuildmat.2013.06.070
28. Kanagaraj, B., Anand, N., Samuvel Raj, R., Lubloy, E. (2022), *Performance evaluation on engineering properties of sodium silicate binder as a precursor material for the development of cement-free concrete*, Devel. Built Environ. 12: 100092. doi: 10.1016/j.dibe.2022.100092
29. Castel, A., Foster, S.J. (2015), *Bond strength between blended slag and Class F fly ash geopolymer concrete with steel reinforcement*, Cem. Concr. Res. 72: 48-53. doi: 10.1016/j.cemconres.2015.02.016
30. Hassan, A., Arif, M., Shariq, M. (2019), *Effect of curing condition on the mechanical properties of fly ash-based geopolymer concrete*, SN Appl. Sci. 1(12): 1694. doi: 10.1007/s42452-019-1774-8
31. Kumar, V., Kumar, P. (2024), *Self-compacted geopolymer concrete incorporating waste ceramic powder*, Multisc. Multidisc. Model. Exp. Des. 7: 5187-5202. doi: 10.1007/s41939-024-00510-7
32. Chokkalingam, P., El-Hassan, H., El-Dieb, A., El-Mir, A. (2022), *Development and characterization of ceramic waste powder-slag blended geopolymer concrete designed using Taguchi method*, Constr. Build. Mater. 349: 128744. doi: 10.1016/j.conbuildmat.2022.128744
33. Karthik, S., Mohan, K.S.R. (2021), *A Taguchi approach for optimizing design mixture of geopolymer concrete incorporating fly ash, ground granulated blast furnace slag and silica fume*, Crystals, 11(11): 1279. doi: 10.3390/cryst11111279
34. Kanagaraj, A.N.B., Alengaram, U.J., Raj, R.S., et al. (2022), *Performance evaluation on engineering properties and sustainability analysis of high strength geopolymer concrete*, J Build. Eng. 60: 105147. doi: 10.1016/j.jobe.2022.105147
35. EFNARC, 2002. Specification and Guidelines for Self-Compacting Concrete. EFNARC (Feb. 2002). ISBN 0 9539733 4 4
36. Patel, Y.J., Shah, N. (2018), *Study on workability and hardened properties of self compacted geopolymer concrete cured at ambient temperature*, Ind. J Sci. Tehcnol. 11(1): 1-12. doi: 10.17485/ijst/2018/v11i1/117698
37. Das, R., Panda, S., Saumendra Sahoo, A., Panigrahi, S.K. (2024), *Effect of superplasticizer types and dosage on the flow characteristics of GGBFS based self-compacting geopolymer concrete*, Mater. Today: Proc. 103: 11-21. doi: 10.1016/j.matpr.2023.06.339
38. IS 516 : Part 1 : Sec 1 : 2021. Hardened concrete methods of test. Part 1: Testing of Strength of Hardened Concrete. Section 1: Compressive, Flexural, and Split Tensile Strength. Bureau of Indian Standards.
39. Li, X., Ma, X., Zhang, S., Zheng, E. (2013), *Mechanical properties and microstructure of class C fly ash-based geopolymer paste and mortar*, Materials, 6(4): 1485-1495. doi: 10.3390/ma6041485
40. Nath, P., Sarker, P.K. (2014) *Effect of GGBFS on setting, workability and early strength properties of fly ash geopolymer concrete cured in ambient condition*, Constr. Build. Mater. 66: 163-171. doi: 10.1016/j.conbuildmat.2014.05.080
41. Huseien, G.F., Ismail, M., Tahir, M.M., et al. (2018), *Synergism between palm oil fuel ash and slag: Production of environmental-friendly alkali activated mortars with enhanced properties*, Constr. Build. Mater. 170: 235-244. doi: 10.1016/j.conbuildmat.2018.03.031
42. Huseien, G.F., Tahir, M.M., Mirza, J., et al. (2018), *Effects of POFA replaced with FA on durability properties of GBFS included alkali activated mortars*, Constr. Build. Mater. 175: 174-186. doi: 10.1016/j.conbuildmat.2018.04.166
43. Kanagaraj, B., Anand, N., Raj R.S., Lubloy, E. (2024), *Behavioural studies on binary blended high strength self compacting geopolymer concrete exposed to standard fire temperature*, Ain Shams Eng. J, 15(2): 102394. doi: 10.1016/j.asej.2023.102394
44. Muhammad, N., Baharom, S., Ghazali, N.A.M., et al. (2019), *Effect of heat curing temperatures on fly ash-based geopolymer concrete*, Int. J Eng. Technol. 8(12): 15-19. doi: 10.14419/ijet.v8i1.2.24866
45. Paruthi, S., Khan, A.H., Isleem, H.F., et al. (2025), *Influence of silica fume and alccofine on the mechanical performance of GGBS-based geopolymer concrete under varying curing temperatures*, J Struct. Integr. Maint. 10(1): 2447661. doi: 10.1080/24705314.2024.2447661
46. Huseien, G.F., Ismail, M., Tahir, M., et al. (2018), *Performance of sustainable alkali activated mortars containing solid waste ceramic powder*, Chem. Eng. Trans. 63: 673-678. doi: 10.3303/CET1863113
47. Lv, X., Yang, L., Li, J., Wang, F. (2022), *Roles of fly ash, granulated blast-furnace slag, and silica fume in long-term resistance to external sulfate attacks at atmospheric temperature*, Cem. Concr. Compos. 133: 104696. doi: 10.1016/j.cemconcomp.2022.104696
48. Puertas, F., Martínez-Ramírez, S., Alonso, S., Vázquez, T. (2000), *Alkali-activated fly ash/slag cements: Strength behaviour*

and hydration products, Cem. Concr. Res. 30(10): 1625-1632. doi: 10.1016/S0008-8846(00)00298-2
49. Kanagaraj, B., Anand, N., Johnson Alengaram, U., Raj, R.S. (2023), *Engineering properties, sustainability performance and life cycle assessment of high strength self-compacting geopolymer concrete composites*, Constr. Build. Mater. 388: 131613. doi: 10.1016/j.conbuildmat.2023.131613
50. Wilding, M.C., Navrotsky, A. (1998), *The dissolution of silica and alumina in silicate melts: In situ high temperature calorimetric studies*, Neues Jahrbuch für Mineralogie, Abhandlungen, 172(2-3): 177-201. doi: 10.1127/njma/172/1998/177
51. IS 516 : Part 5 : Sec 4 : 2020. Hardened Concrete - Methods of Test. Part 5 Non-Destructive Testing of Concrete. Section 4 – Rebound Hammer Test. Bureau of Indian Standards.
52. Nath, P., Sarker, P.K. (2017), *Flexural strength and elastic modulus of ambient-cured blended low-calcium fly ash geopolymer concrete*, Constr. Build. Mater. 130: 22-31. doi: 10.1016/j.conbuildmat.2016.11.034
53. Chouksey, A., Verma, M., Dev, N., et al. (2022), *An investigation on the effect of curing conditions on the mechanical and microstructural properties of the geopolymer concrete*, Mater. Res. Express, 9(5): 055003. doi: 10.1088/2053-1591/ac6be0
54. Sreenivasulu, C., Guru Jawahar, J., Sashidhar, C. (2018), *Predicting compressive strength of geopolymer concrete using NDT techniques*, Asian J Civ. Eng. 19(4): 513-525. doi: 10.1007/s42107-018-0036-1
55. Meskhi, B., Beskopylny, A.N., Stel'makh, S.A., et al. (2023), *Analytical review of geopolymer concrete: retrospective and current issues*, Materials, 16(10): 3792. doi: 10.3390/ma16103792
56. Rahman, S.K., Al-Ameri, R. (2021), *A newly developed self-compacting geopolymer concrete under ambient condition*, Constr. Build. Mater. 267: 121822. doi: 10.1016/j.conbuildmat.2020.121822
57. Ghafoor, M.T., Fujiyama, C. (2023), *Mix design process for sustainable self-compacting geopolymer concrete*, Heliyon, 9(11): e22206. doi: 10.1016/j.heliyon.2023.e22206
58. Huseien, G.F., Sam, A.R.M., Shah, K.W., Mirza, J. (2020), *Effects of ceramic tile powder waste on properties of self-compacted alkali-activated concrete*, Constr. Build. Mater. 236: 117574. doi: 10.1016/j.conbuildmat.2019.117574
59. Huseien, G.F., Ismail, M., Tahir, M., et al. (2018), *Effect of binder to fine aggregate content on performance of sustainable alkali activated mortars incorporating solid waste materials*, Chem. Eng. Trans. 63: 667-672. doi: 10.3303/CET1863112
60. Nazari, A., Bagheri, A., Riahi, S. (2011), *Properties of geopolymer with seeded fly ash and rice husk bark ash*, Mater. Sci. Eng.: A, 528(24): 7395-7401. doi: 10.1016/j.msea.2011.06.027